

# Decentralized Planning of Energy Demand for the Management of Robustness and Discomfort

Evangelos Pournaras, Matteo Vasirani, Robert E. Kooij, and Karl Aberer

**Abstract**—The robustness of smart grids is challenged by unpredictable power peaks or temporal demand oscillations that can cause blackouts and increase supply costs. Planning of demand can mitigate these effects and increase robustness. However, the impact on consumers in regards to the discomfort they experience as a result of improving robustness is usually neglected. This paper introduces a decentralized agent-based approach that quantifies and manages the tradeoff between robustness and discomfort under demand planning. Eight selection functions of plans are experimentally evaluated using real data from two operational smart grids. These functions can provide different quality of service levels for demand-side energy self-management that capture both robustness and discomfort criteria.

**Index Terms**—Demand, discomfort, planning, robustness, smart grid, tree topology.

## I. INTRODUCTION

THE MAIN operational objective of smart grids is to match energy supply and demand. The extent to which supply can meet demand or demand can be adjusted to certain supply is an indication of network and system *robustness*. Demand-side energy management plays a crucial role in robustness as micro-generation via distributed renewable energy resources and technologies such as electrical vehicles make matching supply and demand challenging [1]–[3]. Yet, in demand-side energy management, robustness by itself cannot capture the dynamics of smart grids. Robustness has an impact on human factor that is often neglected or under-emphasized [3]–[6].

This paper claims that improving robustness via demand-side energy management causes a level of discomfort for consumers. The discomfort cost that consumers experience in order to realize a more robust smart grid is referred to as

Manuscript received November 05, 2013; revised March 04, 2014 and May 8, 2014; accepted June 10, 2014. Date of publication June 20, 2014; date of current version November 04, 2014. This work was supported in part by the Netherlands Organisation for Scientific Research (NWO) project RobuSmart under Grant 647.000.001, and in part by the FP7 European project Wattalyst under Grant 288322. Paper no. TII-13-0857.

E. Pournaras is with the Department of Computer Science and Engineering, Faculty of Electrical Engineering, Mathematics, and Computer Science, Delft University of Technology, 2628 CD, Delft, The Netherlands (e-mail: e.pournaras@tudelft.nl).

M. Vasirani and K. Aberer are with the Distributed Information Systems Laboratory, École Polytechnique Fédérale de Lausanne (EPFL), CH-1015, Lausanne, Switzerland (e-mail: vasirani@epfl.ch; karl.aberer@epfl.ch).

R. E. Kooij is with the Department of Computer Science and Engineering, Faculty of Electrical Engineering, Mathematics, and Computer Science, Delft University of Technology, 2628 CD, Delft, The Netherlands, and also with the Netherlands Organisation for Applied Scientific Research, 2628 VK, Delft, The Netherlands (e-mail: r.e.kooij@tudelft.nl).

Digital Object Identifier 10.1109/TII.2014.2332114

*quality of service* under demand-side energy self-management. The goal of this paper is to quantitatively evaluate tradeoffs between robustness and discomfort under demand planning. These tradeoffs can be managed via selections performed by agents that plan the demand of consumers. The performance of different selection schemes is experimentally evaluated with real data from two operational smart grids. Results show that quality of service, with respect to robustness and discomfort, is manageable.

This paper is outlined as follows. Section II illustrates the main concepts of decentralized demand planning. Section III illustrates the plan generation process. Section IV outlines how local and coordinated selections of plans is performed. Section V shows how robustness and discomfort are computed. It also illustrates how the data of two smart grid projects are used in the experimental evaluation that follows in Section VI. Finally, Section VII concludes this paper and outlines future work.

## II. ROBUSTNESS VERSUS DISCOMFORT IN DEMAND PLANNING

*Demand planning* of a consumption source is defined in this paper as the computation of a time series with the amount of energy intended for consumption by this source in a future period of time  $T$ . Consumption sources in demand-side energy management can be defined at different aggregation levels. For example, the household appliance, the wall outlet, the meter of a house, or even the feeder of a neighborhood are all different aggregation levels at which demand can be planned. For simplicity, this paper studies demand planning at the level of household meters; yet, the approach illustrated in this paper can be extended to other aggregation levels as well.

Planning of demand can be applied as a proactive approach for creating a more homogeneous demand curve via *load-shifting* and/or *load-adjustment*. The former action shifts load from high peak times to low peak times without a significant influence in the average load over time [4]. The latter action decreases (or increases) average load via, e.g., incentives mechanisms [5]. Both types of action can be applied to improve robustness by preventing disruptions, such as blackout events, or minimize their impact in case they occur [7]. They can also be used for a more efficient utilization of energy resources, e.g., renewables [8].

On the other hand, *discomfort* refers to the impact that consumers experience on their lifestyle by load-shifting and load-adjustment performed to obtain a higher robustness. This paper distinguishes two types of discomfort that consumers

may experience *shifting discomfort* and *adjustment discomfort*. Shifting discomfort is related to the inconvenience experienced by load-shifting. For example, if planned demand suggests the availability of warm water for showering at later or earlier time than the intended one, this is an indication of discomfort. Adjustment discomfort is related to the inconvenience experienced by load-adjustment. For example, if planned demand suggests lower demand than the intended one for heating during winter, this is an indication of discomfort. However, if the planned demand is higher than the intended one, this is an indication of negative discomfort, assumed to be perceived as comfort. Section V shows how discomfort can be computed in the context of two operational smart grid projects.

Demand-side energy management is often performed in a centralized fashion with utilities companies having a significant level of control in demand planning. This approach raises several issues related to scalability and privacy. Costly investments in computing resources are required by utility companies in order to store and process a large amount of streaming data originated by consumers [9]. Moreover, detailed information about household demand can be used to extract information about the lifestyle of consumers resulting in violation of their privacy [10]. This paper studies an alternative decentralized approach for demand-side self-management: software agents represent the demand preferences of consumers, control their demand by generating a set of *possible plans*  $\mathbf{P}_i = \{\mathbf{p}_i^1, \dots, \mathbf{p}_i^l\} \forall$  agent  $i$ , and specify the *selected plan*  $s_i \in \mathbf{P}_i$  for execution according to criteria defined by a selection function. Possible plans are actually alternative demand time series for the same future period of time.

Agents can generate two types of possible plans in regards to the discomfort that these plans cause to consumers when executed: 1) *equivalent*; and 2) *nonequivalent* possible plans.

Equivalent possible plans are assumed to have a similar impact on the discomfort of consumers. In contrast to lighting sources or television, generating equivalent possible plans is feasible for thermostatically controlled appliances whose operation can be planned without significant disturbance in the lifestyle of consumers [11].

However, possible plans can be nonequivalent as they may cause different levels of discomfort, e.g., possible plans with varied level of average demand (over the planning time). This paper focuses on planning of demand based on nonequivalent possible plans. By adopting nonequivalent possible plans, two opposing objectives need to be met: *maximizing robustness of smart grids while minimizing discomfort that consumers experience*. If consumers need to decrease their demand as a response to a power peak that threatens the stability of smart grids, discomfort is unavoidably increased.

### III. PLAN GENERATION

Fig. 1 illustrates the concept of the plan generation illustrated in this section. Possible plans can be locally generated by clustering historical demand data. Clustering groups time series demand data sampled every certain time period, e.g., every day, for a total period of time, e.g., a week or a month. Grouping is based on the computation of a proximity metric such as the Euclidean or the Manhattan distance [12].

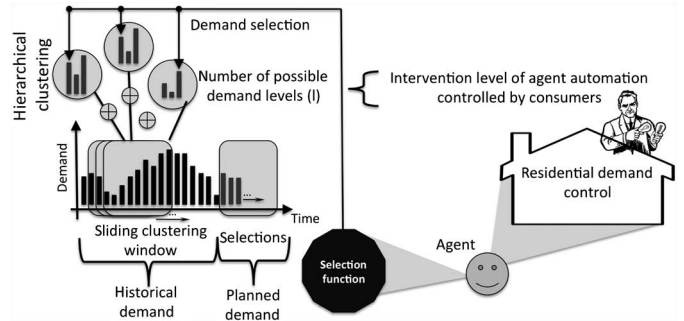


Fig. 1. Plan generation based on historical demand data.

The number of clusters is usually part of the clustering parameterization and represents the number of possible plans that agents generate.

The total period of time from which historic data are used as input in clustering can be defined by a *sliding clustering window*. For example, the California ISO (CAISO) demand forecasting methodology predicts demand based on the energy consumption of the past 10 days [13]. The same principle can be adopted for the generation of possible plans in a following day [14].

Each possible plan is devised by computing the representative demand time series of each cluster. More specifically, each possible plan is the medoid of a cluster and is computed by the median of the historical time series that belongs to this cluster. In clustering, the centroid, computed by the mean, is often employed as the center of clusters. However, this paper considers the centroid as not appropriate for demand planning. The centroid is a computed time series that is not necessarily included in the input historical demand data. The historic demand can be used to reason that the centroid is actually a nonpossible plan as consumers have not necessarily devised such a demand configuration before via their consumption devices. In contrast, the medoid is a plan that is in theory achievable as it corresponds to a consumption pattern observed in the historical consumption data, and therefore, it is a repetition of an earlier consumption pattern. This approach can be extended to capture temporal constraints. For example, if in the next 3 h the consumption should not exceed a certain value, then the medoids that do not meet this constraint can be excluded from the plan generation.

A critical aspect in the clustering process is the number of clusters  $l$  that corresponds to the number of possible plans. Previous experimental work shows that a higher number of possible plans in demand-side energy management results in improved robustness for smart grids [11], [15]. A higher number of possible plans means that agents have a higher degree of freedom to adjust demand according to system objectives. However, a higher number of possible plans increases computational cost<sup>1</sup> and causes a lower cluster size on average. A cluster with a lower size results in a devised possible plan that is less representative of the past energy consumption. This effect is interpreted as providing a higher level of authority to

<sup>1</sup>The increased computational cost concerns the generation process, but also the optimization performed by EPOS as illustrated in Section IV.

agents to autonomously reason about the level of household demand and is referred to in this paper as the *intervention level* of home automation technologies for demand planning. The intervention level  $I_i^j$  of a possible plan  $j$  generated by agent  $i$  is defined as follows:

$$I_i^j = 1 - \frac{C_i^j}{\sum_{p=1}^l C_i^p} \quad (1)$$

where the relative cluster size is computed by the size of the cluster  $C_i^j$ ,  $j \in \{1, \dots, l\}$  and the sum  $\sum_{p=1}^l C_i^p$  of the total number of historic time series sampled for clustering.

#### IV. PLAN SELECTION

Agents select and execute one of their possible plans to meet different system objectives of smart grids. Two types of agent selections are distinguished in this paper: 1) *local*; and 2) *coordinated* selections.

A local selection of an agent is independent of other agent selections. For example, selecting the plan with the minimum average energy consumption is a local selection that each agent can perform individually without exchanging information with other agents. However, for more complex system objectives related to load-shifting, agent selections are interdependent and coordination between agents is required.

Centralized coordination is not a scalable approach as the complexity for computing the optimum combination of agent selections is exponential. More specifically, in a network of  $n$  agents with  $l$  number of possible plans per agent, the complexity of a brute-force operation is  $O(l^n)$ . A brute-force operation computes the sum of all combinations between the possible plans of agents. The sum of each combination computed by an agent  $i$  is referred to as the *combinational plan*  $c_i^j$ . This paper focuses on large-scale decentralized coordination of agent selections using the *Energy Plan Overlay Self-stabilization system* (EPOS) [11], [15]. In EPOS, agents are organizationally structured in a tree topology through which they interact and coordinate their selections as shown in Fig. 2. EPOS decreases computational complexity to  $O(l^c)$ , where  $c$  is the number of children per agent for a  $c$ -ary tree. Fault tolerance can be provided with self-organization mechanisms such as adaptive epidemic tree overlay service (AETOS) [16] that builds and maintains reconfigurable tree topologies in dynamic distributed environments.

Coordination in EPOS is performed in bottom-up consecutive *coordination steps* between children and their parents. During a coordination step, the children of a tree level provide to their parents their possible plans together with the summation of all selections performed in the branch underneath. For each agent  $i$  with  $c$  children, this summation is the *aggregate plan*  $\mathbf{a}_i = \sum_{v=1}^c \mathbf{a}_v = \sum_{h \in |\mathbf{B}_i|} \mathbf{s}_h \forall$  agent  $h$  belonging to the branch  $\mathbf{B}_i$  underneath agent  $i$ . The possible and aggregate plans are input in a selection function. The output of the selection function indicates the selected plan of each child. The process of consecutive coordination steps repeats up to the root that broadcasts to each agent  $i$  the *global plan*  $\mathbf{g} = \sum_{i=1}^n \mathbf{s}_i$  of the system that is the summation of all agent selections. The broadcast completes the *coordination phase* after which

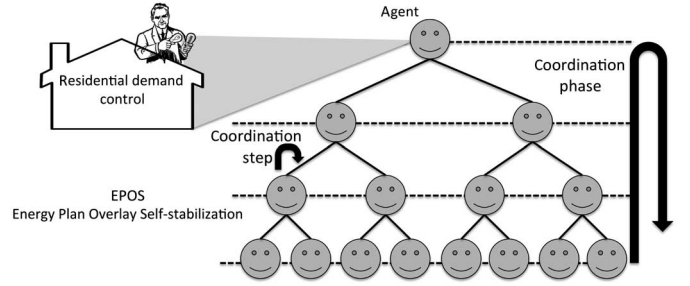


Fig. 2. Agents of EPOS structured in a tree topology to coordinate their plan selection.

TABLE I  
SELECTION FUNCTIONS FOR DEMAND-SIDE ENERGY MANAGEMENT

	Selection Function	Definition
Local Selections	RANDOM:	$\arg \text{rand}(\mathbf{p}_i^j)$
	MIN-DEMAND:	$\arg \min_{j=1}^l \{\text{avg}(\mathbf{p}_i^j)\}$
	MAX-DEMAND:	$\arg \max_{j=1}^l \{\text{avg}(\mathbf{p}_i^j)\}$
	MIN-INTERVENTIONS:	$\arg \min_{j=1}^l (I_j)$
Coordinated Selections	MIN-DEVIATIONS:	$\arg \min_{j=1}^{l^c} \{\sigma(\mathbf{a}_i + \mathbf{c}_i^j)\}$
	MIN-RELATIVE-DEVIATIONS:	$\arg \min_{j=1}^{l^c} \left\{ \frac{\sigma(\mathbf{a}_i + \mathbf{c}_i^j)}{\text{avg}(\mathbf{a}_i + \mathbf{c}_i^j)} \right\}$
	MAX-LOAD-FACTOR:	$\arg \max_{j=1}^{l^c} \left\{ \frac{\text{avg}(\mathbf{a}_i + \mathbf{c}_i^j)}{\max(\mathbf{a}_i + \mathbf{c}_i^j)} \right\}$
	MAX-ENTROPY <sup>*</sup> :	$\arg \max_{j=1}^{l^c} \left( - \sum_{t=1}^T u_i^t \log u_i^t \right)$

\*  $u_i^t = \frac{a_i^t + c_i^t}{\sum_{t=1}^T (a_i^t + c_i^t)}$  is the demand utilization at planning time  $t$ .

each selected plan  $\mathbf{s}_i$  can be executed. More details about the algorithm execution and the agent interactions are illustrated in earlier work [11], [15].

This paper studies and evaluates the selection functions of Table I. The functions that perform local selections receive as input local information such as each possible plan  $\mathbf{p}_i^j$  and intervention level  $I_i^j$ . MAX-DEMAND and MIN-DEMAND are the actual upper and lower bound of demand adjustment. They also represent the maximum adjustment comfort and discomfort that consumers can experience, respectively, as illustrated in Section V. The functions for coordinated selections receive the aggregate plan  $\mathbf{a}_i$  and each combinational plan  $\mathbf{c}_i^j$  for input. The homogeneity of the planned demand over time is captured by these functions with various metrics such as the standard deviation (MIN-DEVIATIONS), the relative standard deviation (MIN-RELATIVE-DEVIATIONS), the load factor [17] (MAX-LOAD-FACTOR), and the entropy [6] (MAX-ENTROPY).

For the purpose of this paper, the functionality of EPOS is significantly extended. More specifically, the contributions of this paper to EPOS are the following: 1) scope extension from the aggregation level of single devices to the aggregation level of household; 2) scope extension from equivalent to nonequivalent possible plans; 3) introduction of several other selection functions besides MIN-DEVIATIONS and REVERSING-DEVIATIONS [11], [15]; and 4) evaluation of EPOS using real data from operational smart grids instead of synthetic data.

## V. VALIDATION IN SMART GRID PROJECTS

The actual robustness and discomfort that consumers experience via demand planning are validated *a posteriori* using real consumption data from two operational smart grid projects, the *Electricity Customer Behavior Trial*<sup>2</sup> in Ireland and the *Olympic Peninsula Smart Grid Demonstration*<sup>3</sup> in the USA. The data of the projects are referred to in this paper as CONTROL-DATA  $\mathbf{d}$  and are used for generating possible plans and making quantitative comparisons with the global plan  $\mathbf{g}$ .

The possible plans of agents are generated by clustering time series consumption data of the past 10 days that is the length of the sliding clustering window. The number of plans is selected based on two different criteria: 1) statically by assigning a default number of plans to each agent; and 2) dynamically by computing the number of plans based on project data. In the former case, the minimum number of  $l = 2$  is selected. This number minimizes the intervention level and the computational cost in each agent. In the latter case, the number of possible plans is computed by letting agents reason about the preferences of consumers based on selections they made in the context of each project, e.g., survey answers and temperature setpoints.

A robustness metric is introduced in this paper to compare the demand homogeneity achieved with each selection function. Robustness can be quantified by the distance of each demand value in the computed global plan  $\mathbf{g}$  from its average  $\text{avg}(\mathbf{g})$  that represents the optimum “flat” demand curve. This distance can be compared with the respective distance of CONTROL-DATA  $\mathbf{d}$ . The robustness  $R$  between the two demand curves is computed by the mean-square error as follows:

$$R = \frac{1}{T} \sum_{t=1}^T \rho^t \quad (2)$$

where

$$\rho^t = \begin{cases} (\hat{g}^t - \hat{d}^t)^2, & \text{if } \hat{g}^t \geq \hat{d}^t \\ -(\hat{g}^t - \hat{d}^t)^2, & \text{if } \hat{g}^t < \hat{d}^t \end{cases} \quad (3)$$

and

$$\hat{g}^t = 1 - \frac{|g^t - \text{avg}(\mathbf{g})|}{\text{avg}(\mathbf{g})} \quad \text{and} \quad \hat{d}^t = 1 - \frac{|d^t - \text{avg}(\mathbf{d})|}{\text{avg}(\mathbf{d})}. \quad (4)$$

Normalization is performed to remove information about the level of demand between the global plans formed by different selection functions. A robustness value by itself cannot indicate quantitatively the homogeneity of a selection function. Normalization provides more unbiased relative comparisons between different selection functions and a better distinction of robustness from the following discomfort metrics that capture the different demand levels rather than the homogeneity.

Shifting discomfort is computed by the root-mean-square error between the selected plans and CONTROL-DATA for each agent  $i$

$$D_s = \sum_{i=1}^n \left\{ w_i^s \sqrt{\frac{1}{T} \sum_{t=1}^T (s_i^t - d_i^t)^2} \right\}. \quad (5)$$

The weight  $w_i^s$  of each agent  $i$  quantifies the interest of each consumer for load-shifting. A high value of  $w_i^s$  shows that a consumer is not so self-interested in load-shifting or the impact of shifting discomfort is perceived more “negative” compared to consumer with a low  $w_i^s$ . The value of this weight is selected in the context of the smart grid projects illustrated in the rest of this section.

Adjustment discomfort is computed by summing positive and negative errors between the selected plans and CONTROL-DATA for each agent  $i$

$$D_a = \sum_{i=1}^n w_i^a \sum_{t=1}^T (s_i^t - d_i^t). \quad (6)$$

The weight  $w_i^a$  of each agent  $i$  is related with how “negative” different consumers perceive the adjustment discomfort due to demand reduction. Similarly to  $w_i^s$ , the values of  $w_i^a$  are selected within the context of the smart grid projects.

### A. Electricity Customer Behavior Trial Project

This project is a cost-benefit analysis that assesses the impact on electricity consumption of consumers in Ireland. The project ran in the period 2009–2010 with 5000 residential and business consumers participating. The data are cleaned from missing values and filtered out to contain the energy consumption time series of 782 residential consumers that belong to the control group.<sup>4</sup>

Agents reason about the number of possible plans based on the following two questions<sup>5</sup>:

**Question 1.** *My household may decide to make minor changes to the way we use electricity.*

**Question 2.** *My household may decide to make major changes to the way we use electricity.*

The answer  $a_q$  in each of the above question  $q$  belongs to  $\{1, \dots, 5\}$ , where 1 stands for a strong agreement and 5 stands for a strong disagreement. Table IV of Appendix A illustrates how agents reason about the number of possible plans they generate.<sup>6</sup> The number of plans computed by this algorithm is referred to in this paper as  $l = f_1(z = x)$ . The main intuition behind the generation algorithm is the normalization of the answers to the two questions  $a_1$  and  $a_2$  in

<sup>4</sup>These consumers are not affected by the dynamic pricing schemes applied for the purpose of the project.

<sup>5</sup>The question block “55122” of the pretrial residential survey contains these two questions.

<sup>6</sup>From the total number of 782 residential consumers, 132 of these do not participate in the pretrial survey. For 116 of these consumers, the question block “54132” of the posttrial survey is used for computing Table IV. This question block is the respective posttrial question block “55122” of the pretrial survey. (*My household made minor/major changes to the way we use electricity.*) For the final 16 residential consumers that do not participate in neither of the pretrial nor posttrial surveys, the number of possible plans is computed by the median number of possible plans in the the rest of the 766 consumers.

<sup>2</sup>Available: <http://www.ucd.ie/issda/data/commissionforenergyregulationcer/> (last accessed September 2013).

<sup>3</sup>Available: <http://svn.pnl.gov/olyphen/> (last accessed September 2013).

$l \in \{z-2, \dots, z+3\}$ . The constant  $z$  is used as a scaling factor for the number of possible plans in the generation process.

The weights of discomfort are computed by the answers of consumers to the following two questions:

**Question 3.** *I am interested in changing the way I use electricity if it helps environment.*<sup>7</sup>

**Question 4.** *It is too inconvenient to reduce our usage of electricity.*<sup>8</sup>

Based on the possible answers  $\{1, \dots, 5\}$ , where 1 stands for a strong agreement and 5 stands for a strong disagreement, the weights  $w_i^s$  and  $w_i^a$  for each agent  $i$  are computed by normalizing the answers in the range  $[0, 1]$ .

### B. Olympic Peninsula Smart Grid Demonstration Project

This project assesses the adjustment of individual energy use based on price signals exchanged within a two-way bidding market [18]. The project concerns the period of March 2006–March 2007 with 112 household participants regionally distributed in the Olympic Peninsula of the USA. The data subset from November 2006 to March 2007 is selected during which the fewest number of missing values is observed. The demand of each consumer is captured every 5 min. Demand data are aligned to the sampling rate of the Electricity Customer Behavior Trial project by aggregating 12 consecutive demand bids of each hour to a single hourly demand bid.

Demand data are filtered out to contain 29 consumers that either belong to the CONTROL group or have a FIXED type of contract and have lower than 20% of their values missing. Two extra consumers are excluded as their demand time series containing a large proportion of zero values. Therefore, the final number of consumers used is 27. The missing values in the final consumers are interpolated by computing the average demand values in the past and future 10 days.

In the context of this project, the demand adjustment is achieved by dynamically modifying the temperature setpoints of various household devices. Motivated by this approach, the number of possible plans  $l = f_2(z = x)$  is defined by a function that captures the selected temperature setpoints of consumers during project runtime. More specifically, the range of minimum and maximum temperature setpoints selected is normalized to  $l \in \{z, \dots, z + 4\}$  for a given constant  $z$ .

This project contains a significantly lower number of participants than the Electricity Customer Behavior Trial project resulting in a low statistical significance in the illustrated results. Most demonstration projects are small in scale and it is challenging to validate demand-side energy management mechanisms in large-scale systems. Nonetheless, this project provides a second confirmation of the findings of this paper. It also shows how the clustering methodology illustrated in this paper can be applied in different projects, e.g., how the number of possible plans can be computed in two different ways in the context of each project: survey questions or choices of temperature setpoints.

<sup>7</sup>This is question “4331” in the residential pretrial survey.

<sup>8</sup>This is question “4352” in the residential pretrial survey.

## VI. EXPERIMENTAL EVALUATION

This section quantitatively evaluates the tradeoff between robustness and discomfort under different selection functions. An implementation of the hierarchical clustering algorithm [19] in Weka<sup>9</sup> is used for generating the possible plans of agents. Two  $z$  values are evaluated for each project<sup>10</sup>:  $z = 2$ ,  $z = 3$  for the Electricity Customer Behavior Trial project and  $z = 1$ ,  $z = 2$  for the Olympic Peninsula Smart Grid Demonstration project. The first choices of  $z = 2$  and  $z = 1$  for each project bound the lowest values of  $l$  to the minimum values of 0 and 1. The second choices of  $z = 3$  and  $z = 2$  shift the distribution by 1. The normalized histograms for each  $z$  value and weights of discomfort are shown in Appendix A.

Agents are engineered as distributed application of Protopeer [20] that is a prototyping toolkit for large-scale distributed systems. Agents perform local selections or coordinated ones by implementing EPOS in Protopeer as well. Each coordination phase of EPOS runs for 10 different 3-ary tree topologies. Each topology is built by the AETOS overlay service [16]. AETOS self-organizes agents in different random positions for each tree topology to capture the effect of topological positioning. The effect of different types of tree topologies is evaluated in earlier work [21], [15]. Each coordination phase of EPOS concerns a random day of the week and simulates one demand–response event.

### A. Robustness Versus Discomfort

Tables II and III summarize the performance of the selection functions in each project. The data illustrated concern the average of the total period of time studied in each project. Performance is measured by the three metrics introduced in this paper: 1) robustness; 2) shifting discomfort; and 3) adjustment discomfort. Three planning generation schemes are evaluated in each project, one static with  $l = 2$  and two dynamic.

Robustness improves for every selection function that performs coordinated selections in both projects and every generation scheme. The highest improvement is achieved by the MAX-ENTROPY and MIN-RELATIVE-DEVIATIONS. MIN-INTERVENTIONS does not have a significant influence on robustness. As the average number of possible plans increases more than  $l = 2$ , robustness also increases in average 52%, for  $l = f_1(z = 2)$ ; 61% for  $l = f_1(z = 3)$ ; 30%, for  $l = f_2(z = 1)$ ; and 39%, for  $l = f_2(z = 2)$ , confirming earlier findings concerning equivalent possible plans [11], [15].

Shifting discomfort maximally decreases under MIN-INTERVENTIONS and MIN-DEMAND. MAX-DEMAND, MAX-ENTROPY, and RANDOM cause the highest shifting discomfort. The high robustness of MAX-ENTROPY is actually achieved through an increase in shifting discomfort. The lowest shifting discomfort under coordinated selections is achieved by MIN-DEVIATIONS. Compared to  $l = 2$ , shifting discomfort is influenced by the increase in the number of possible plans

<sup>9</sup>Available: <http://www.cs.waikato.ac.nz/ml/weka/> (last accessed September 2013).

<sup>10</sup>If  $l \leq 1$ , then agents select the median time series from the historic sliding window.

TABLE II  
 PERFORMANCE OVERVIEW FOR THE ELECTRICITY CUSTOMER BEHAVIOR TRIAL PROJECT

	Selection Function	$R (x * 10^{-3})$			$D_s$			$D_a$			
		$l$ :	2	$f_1(z=2)$	$f_1(z=3)$	2	$f_1(z=2)$	$f_1(z=3)$	2	$f_1(z=2)$	$f_1(z=3)$
Local Selections	RANDOM:		-0.50	-0.08	0.08	83.11	81.75	82.08	-349.64	-327.46	-311.32
	MIN-DEMAND:		2.72	5.08	6.68	66.90	67.51	68.07	821.63	1053.52	1187.48
	MAX-DEMAND:		-5.37	-5.31	-5.65	99.42	96.48	97.39	-1516.07	-1679.63	-1809.30
	MIN-INTERVENTIONS:		0.98	1.17	1.08	65.74	66.59	67.68	594.17	609.74	586.83
Coordinated Selections	MIN-DEVIATIONS:		7.79	14.28	19.18	69.03	69.51	70.18	614.72	752.65	830.76
	MIN-REL-DEVIATIONS:		9.23	16.22	21.11	74.26	74.02	74.83	143.83	169.42	196.09
	MAX-LOAD-FACTOR:		4.83	8.17	10.68	79.30	79.30	79.30	-188.86	-188.86	-235.40
	MAX-ENTROPY:		9.64	22.05	22.04	99.42	99.42	99.42	-1516.07	-1516.07	-1516.07

 Low performance  High performance

 TABLE III  
 PERFORMANCE OVERVIEW FOR THE OLYMPIC PENINSULA SMART GRID DEMONSTRATION PROJECT

	Selection Function	$R (x * 10^{-3})$			$D_s$			$D_a$			
		$l$ :	2	$f_2(z=1)$	$f_2(z=2)$	2	$f_2(z=1)$	$f_2(z=2)$	2	$f_2(z=1)$	$f_2(z=2)$
Local Selections	RANDOM:		21.57	47.99	47.13	47.40	40.54	42.08	-108.95	-80.56	-96.92
	MIN-DEMAND:		-2.83	33.28	17.60	38.32	33.57	34.15	119.27	153.76	191.33
	MAX-DEMAND:		38.37	55.34	60.51	57.03	48.18	51.37	-338.55	-314.20	-405.29
	MIN-INTERVENTIONS:		-11.36	46.76	36.68	38.59	32.19	32.60	90.26	87.86	95.12
Coordinated Selections	MIN-DEVIATIONS:		70.97	113.13	133.68	39.54	34.37	35.06	73.98	91.31	111.62
	MIN-REL-DEVIATIONS:		127.38	138.38	168.16	46.0	39.48	41.09	-123.49	-95.60	-117.12
	MAX-LOAD-FACTOR:		112.07	119.80	152.95	47.12	41.04	41.49	-136.66	-110.16	-113.85
	MAX-ENTROPY:		123.53	134.24	165.85	45.09	39.39	40.41	-97.74	-96.14	-103.80

 Low performance  High performance

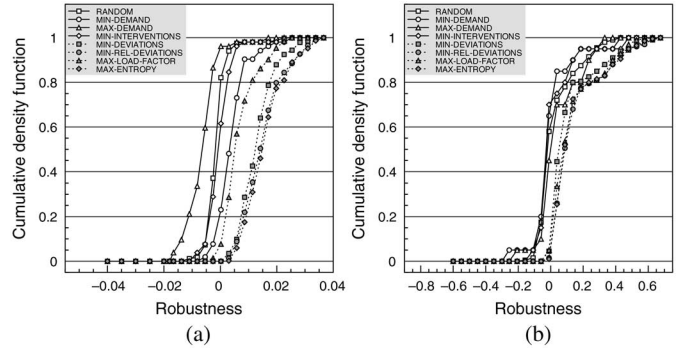
as follows: 1) 0.4% average increase for  $l = f_1(z=2)$ ; 2) 0.3% average decrease for  $l = f_1(z=3)$ ; 3) 14% average increase for  $l = f_2(z=1)$ ; and 4) 11.4% average increase for  $l = f_2(z=2)$ .

Adjustment discomfort maximally decreases under MAX-DEMAND and MAX-ENTROPY. MIN-DEMAND and MIN-DEVIATIONS cause the highest adjustment discomfort. The high robustness of MIN-DEVIATIONS is achieved through an increase in adjustment discomfort, in contrast to MAX-ENTROPY that achieves high robustness by increasing shifting discomfort. The increase in the number of possible plans influences adjustment discomfort as follows: 1) 19% average increase for  $l = f_1(z=2)$ ; 2) 23% average increase for  $l = f_1(z=3)$ ; 3) 30.3% average increase for  $l = f_2(z=1)$ ; and 4) 15.9% average increase for  $l = f_2(z=2)$ .

This section also illustrates the cumulative distribution functions of robustness and discomfort for each selection function and project. A cumulative distribution function  $F_X(x) = \Pr(X \leq x)$  for  $X = R, D_s$ , or  $D_a$  shows how robustness and discomfort are distributed during the runtime of the projects. Therefore, they provide detailed observations compared to the results of Tables II and III. Cumulative distribution functions focus on  $f_1(z=2)$  and  $f_2(z=2)$ .

Fig. 3 illustrates the cumulative distribution functions of robustness for the two projects. The selection functions that perform coordinated selections are shifted to positive robustness values, whereas local selections and especially MAX-DEMAND are shifted toward negative robustness values. The Electricity Customer Behavior Trial project concerns data of a higher number of consumers and a longer period of time than the Olympic Peninsula Smart Grid Demonstration project. This explains the higher overlap of the cumulative distribution functions in the second project.

Fig. 4 illustrates the cumulative distribution functions of shifting discomfort for the two projects. MIN-INTERVENTIONS


 Fig. 3. Cumulative distribution functions of robustness  $R$  for  $z = 2$ . (a) Electricity Customer Behavior Trial project. (b) Olympic Peninsula Smart Grid Demonstration project.

and MIN-DEMAND are positioned to values of lower shifting discomfort in contrast to MAX-DEMAND that is clearly positioned to higher values. The selection functions that perform coordinated selections are positioned to higher values compared to MIN-INTERVENTIONS and MIN-DEMAND.

Fig. 5 shows that under local selections, the cumulative distribution functions of adjustment discomfort are shifted to negative values, yet, MIN-INTERVENTIONS and MIN-DEMAND cause adjustment discomfort and that is why their distributions are shifted to positive values. Under coordinated selections, the distributions vary significantly, with MAX-LOAD-FACTOR and MAX-ENTROPY shifted to negative values that cause comfort to consumers, whereas the rest of the selection functions are mainly located between positive and negative values.

This observation can be explained by the fact that coordinated selections acquire a flat demand curve by either increasing or decreasing the average demand, e.g., January 19, 2010 and May 28, 2010, respectively, for the Electricity Customer Behavior Trial project. Therefore, adjustment discomfort is

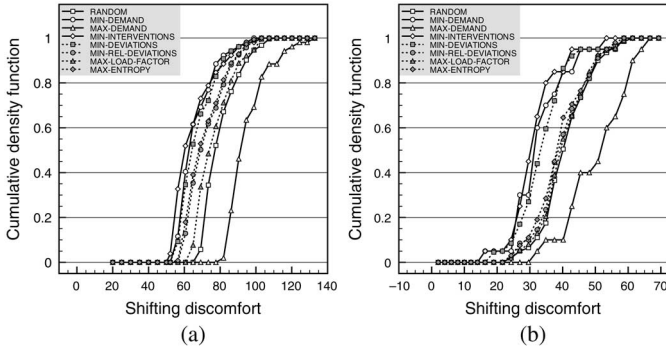


Fig. 4. Cumulative distribution functions of shifting discomfort  $D_s$  for  $z = 2$ . (a) Electricity Customer Behavior Trial project. (b) Olympic Peninsula Smart Grid Demonstration project.

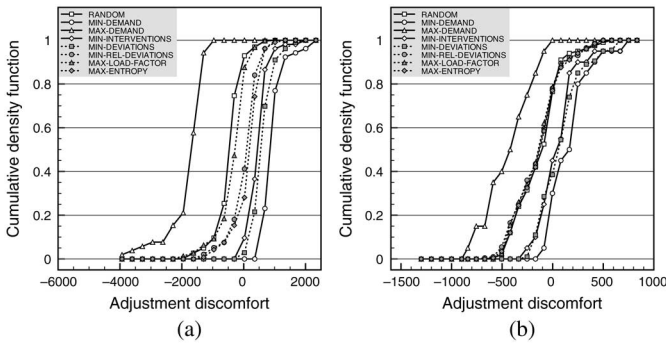


Fig. 5. Cumulative distribution functions of adjustment discomfort  $D_a$  for  $z = 2$ . (a) Electricity Customer Behavior Trial project. (b) Olympic Peninsula Smart Grid Demonstration project.

highly influenced by temporal factors related to the weather and different choices that consumers make in different seasons of a year. The demand curves in Section VI-B confirm this explanation.

*B. Demand Curves*

Fig. 6 illustrates the demand curves of CONTROL-DATA and the global plans of each selection function on January 19, 2010 and May 28, 2010 under  $l = 2$ . These data concern the Electricity Customer Behavior Trial project. CONTROL-DATA has two main demand peaks, one low peak in the morning between 06:00 and 08:00 and one high peak in the evening between 17:00 and 21:00. The morning peak is more distinguishable on May 28, 2010 than January 19, 2010, whereas the evening peak is higher and more distinguishable in the winter day.

Fig. 7 illustrates the demand curves of CONTROL-DATA and the global plans of each selection function on January 16, 2007 for the Olympic Peninsula Smart Grid Demonstration project. The minimum number of possible plans  $l = 2$  is selected in this case as well. The high winter peak is observed in the morning, with a low evening peak following.

The MAX-DEMAND and MIN-DEMAND in Figs. 6(a), (c), and 7(a) are the upper and lower bounds that form the demand envelope of planning within which the performance of all selection functions lies. MIN-INTERVENTIONS results in plan selections with low energy consumption. This means that

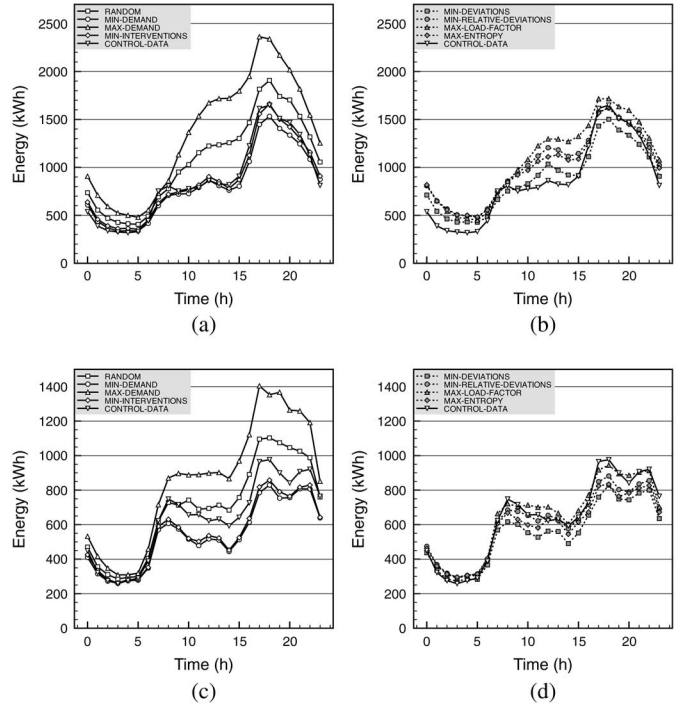


Fig. 6. Actual demand curve and the demand of the global plans for the Electricity Customer Behavior Trial project under  $l = 2$ . (a) Local selection on 19/01/2010. (b) Coordinated selection on 19/01/2010. (c) Local selection on 28/05/2010. (d) Coordinated selection on 28/05/2010.

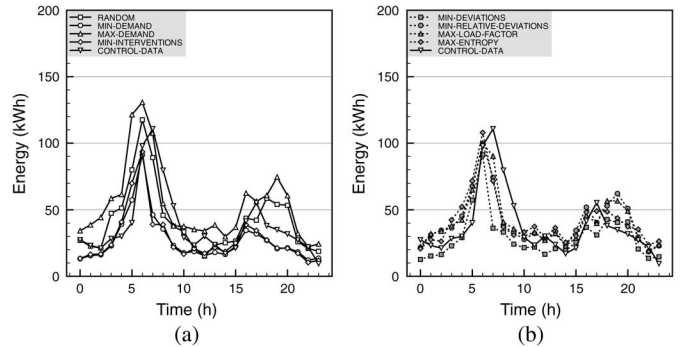


Fig. 7. Actual demand curve and the demand of the global plans for the Olympic Peninsula Smart Grid Demonstration project on January 16, 2007 under  $l = 2$ . (a) Local selection. (b) Coordinated selection.

possible plans with extreme high values are not the cluster with the largest size. In Fig. 6(b) and (d), the global plans are observed above the CONTROL-DATA during most hours on January 19, 2010 compared to May 28, 2010. This means that robustness requires a demand increase for a longer period of time during a winter day compared to a spring day. This demand increase is the actual load-shifting performed to suppress the high power peak. MIN-DEVIATIONS decreases the high peak up to 9% on January 19, 2010 and 16% on May 28, 2010 for the Electricity Customer Behavior Trial project. Respectively, the high peak decreases 44% on January 16, 2007 for the Olympic Peninsula Smart Grid Demonstration project.

### C. Quality of Service

This section shows how performance tradeoffs between robustness and discomfort can determine quality of service in demand-side energy self-management. More specifically, assume that consumers, utility companies or system operators need to choose one of the selection functions that satisfies certain robustness and discomfort criteria. Choice is performed as follows:

$$\arg \max_{o \in \mathbf{F}} = \alpha r_o^r + \beta r_o^s + \gamma r_o^a \quad (7)$$

where  $r_o^r, r_o^s, r_o^a \in [0, 7]$  are the ranks of a selection function  $o \in \mathbf{F} = \{\text{RANDOM, MIN-DEMAND, MAX-DEMAND, MIN-INTERVENTIONS, MIN-DEVIATIONS, MIN-RELATIVE-DEVIATIONS, MAX-LOAD-FACTOR, MAX-ENTROPY}\}$  for the three respective performance metrics: 1) robustness  $R$ ; 2) shifting discomfort  $D_s$ ; and 3) adjustment discomfort  $D_a$ . Ranking is derived by the results of Tables II and III with the value of 0 corresponding to the lowest performance and the value of 7 to the highest performance. The weights  $\alpha$ ,  $\beta$ , and  $\gamma$  indicate the relative “importance” of each performance metric and it holds that  $\alpha + \beta + \gamma = 1$ .

The relation between a certain choice of a selection function and the threshold values of  $\alpha$ ,  $\beta$ , and  $\gamma$ , which result in this selection, can be computed and visualized using decision trees built by the C4.5 algorithm [22]. Learning is performed by a 10-fold cross-validation of a training set generated using (7) with 66 different threshold combinations of  $\alpha$ ,  $\beta$ , and  $\gamma$  under a step-wise increment of 0.1. Each decision tree concerns the aggregate results of all temporal demand data in each project, yet, such trees can be computed for more specific time periods, e.g., seasons or months.

Fig. 8 illustrates the decision tree for the performance results of the Electricity Customer Behavior Trial project. This tree contains two selection functions that perform local selections (MAX-DEMAND and MIN-INTERVENTIONS) and two selection functions that perform coordinated selections (MIN-RELATIVE-DEVIATIONS and MAX-ENTROPY). MAX-DEMAND is chosen when  $\beta \leq 0.3$  and  $\alpha \leq 0.1$ . MIN-INTERVENTIONS is chosen under  $\beta > 0.3$  and  $\alpha \leq 0.3$ . However, for criteria that define high  $\alpha$ , MAX-ENTROPY and MIN-RELATIVE-DEVIATIONS are selected depending on the values of discomfort. In this case, lower adjustment discomfort weights result in choices of MIN-RELATIVE-DEVIATIONS over MAX-ENTROPY.

Fig. 9 illustrates the respective decision tree for the Olympic Peninsula Smart Grid Demonstration project. This tree has lower complexity than the tree of the Electricity Customer Behavior Trial project. It provides choices between three selection functions, MAX-DEMAND, MIN-INTERVENTIONS, and MIN-RELATIVE-DEVIATIONS, which are determined by the shifting discomfort and adjustment discomfort.

### D. Summary of Findings

The main findings of this paper are summarized as follows.

- 1) MAX-ENTROPY and MIN-RELATIVE-DEVIATIONS achieve the highest robustness.

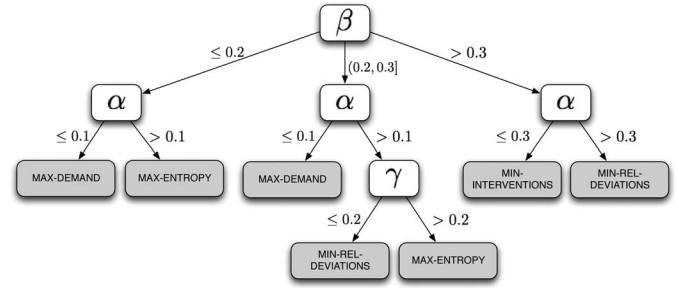


Fig. 8. Decision tree of selection functions for the Electricity Customer Behavior Trial project.

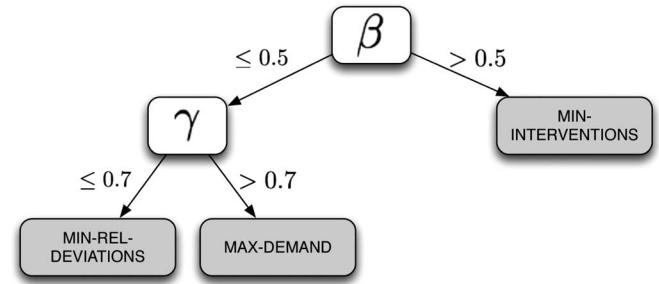


Fig. 9. Decision tree of selection functions for the Olympic Peninsula Smart Grid Demonstration project.

- 2) MIN-INTERVENTIONS achieves the lowest shifting discomfort and MAX-DEMAND the lowest adjustment discomfort.
- 3) MIN-DEVIATIONS achieves the highest peak shavings.
- 4) A higher number of possible plans increases robustness at a cost of higher discomfort.
- 5) Peak shaving is achieved either via an overall demand increase or decrease over time.
- 6) Quality of service under demand planning can be managed by decision trees that compute tradeoffs between robustness and discomfort.

## VII. CONCLUSION AND FUTURE WORK

This paper concludes that the tradeoff between robustness and discomfort in demand-side energy self-management is quantifiable, manageable, and can provide different quality of service levels. More specifically, the experimental validation with real data from two operational smart grid projects confirms the load-shifting and load-adjustment potential of various selection functions, but also their discomfort impact on consumers. These selection functions can become a highly modular element of decentralized demand planning mechanisms such as EPOS [11], [15], in future smart grids. Other factors related to malicious agents and a fair distribution of discomfort between consumers are part of future work.

### ACKNOWLEDGMENT

The authors would like to thank T. K. Wijaya for his software support on clustering. They are also grateful to the Irish Social Science Data Archive and the Pacific Northwest National Laboratory for providing access to power demand data.

TABLE IV  
COMPUTING THE NUMBER OF POSSIBLE PLANS FOR THE ELECTRICITY  
CUSTOMER BEHAVIOR TRIAL PROJECT

Condition	$a_1$	$a_2$	$l$
1	*	1	$z + 3$
2	*	2	$z + 2$
3	*	3	$z + 1$
4	3	4	$z$
5	$< 3$	4	$z + 1$
6	$> 3$	4	$z - 1$
7	3	5	$z - 1$
8	$< 3$	5	$z$
9	$> 3$	5	$z - 2$

The constant  $z$  represents a default value for  $l$ .

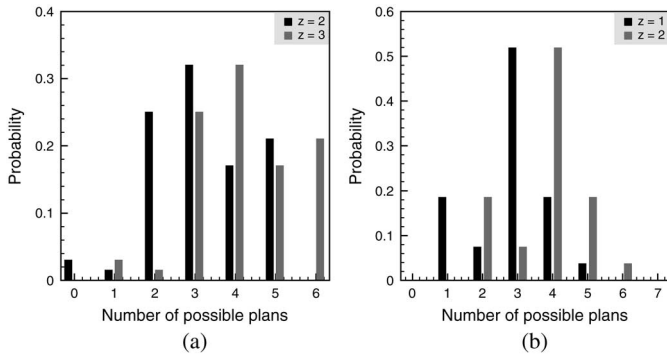


Fig. 10. Normalized histograms for the number of possible plans  $l$ . (a) Electricity Customer Behavior Trial project. (b) Olympic Peninsula Smart Grid Demonstration project.

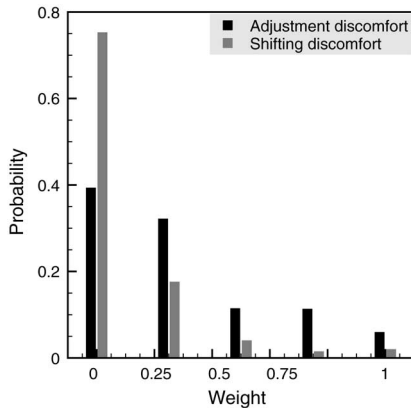


Fig. 11. Normalized histogram of shifting  $w_s^q$  and adjustment  $w_a^q$  discomfort weights derived from the pretrial survey of the Electricity Customer Behavior Trial project.

## APPENDIX A SUPPLEMENTAL MATERIAL

Table IV illustrates how the number of possible plans is generated for the Electricity Customer Behavior Trial project. As consumers tend to agree more to changes in energy consumption, the number of plans also increases. If a consumer chooses in Question 2 for major changes in his/her electricity, then a higher intervention level is introduced by increasing the number of possible plans (e.g., conditions 1–3 in Table IV).

Fig. 10 illustrates the normalized histograms for the number of possible plans  $l$  in the two smart grid projects. These two

histograms are generated according to Table IV using two different values of  $z$ .

Fig. 11 illustrates the normalized histogram for the two weights of discomfort based on the answers of consumers in Question 3 and 4.

## REFERENCES

- [1] P. Siano, "Demand response and smart grids—A survey," *Renew. Sustain. Energy Rev.*, 2014, vol. 30, pp. 461–478.
- [2] P. Palensky and D. Dietrich, "Demand side management: Demand response, intelligent energy systems, and smart loads," *IEEE Trans. Ind. Informat.*, vol. 7, no. 3, pp. 381–388, Aug. 2011.
- [3] G. Strbac, "Demand side management: Benefits and challenges," *Energy Policy*, vol. 36, no. 12, pp. 4419–4426, Dec. 2008.
- [4] M. Stadler, W. Krause, M. Sonnenschein, and U. Vogel, "Modelling and evaluation of control schemes for enhancing load shift of electricity demand for cooling devices," *Environ. Model. Softw.*, vol. 24, no. 2, pp. 285–295, Feb. 2009.
- [5] P. Joskow and J. Tirole, "Reliability and competitive electricity markets," *RAND J. Econ.*, vol. 38, no. 1, pp. 60–84, May 2007.
- [6] H. Aalami, M. P. Moghaddam, and G. Yousefi, "Modeling and prioritizing demand response programs in power markets," *Electr. Power Syst. Res.*, vol. 80, no. 4, pp. 426–435, 2010.
- [7] E. Pournaras, M. Yao, R. Ambrosio, and M. Warnier, "Organizational control reconfigurations for a robust smart power grid," in *Internet of Things and Inter-Cooperative Computational Technologies for Collective Intelligence*. Berlin, Germany: Springer-Verlag, 2012, vol. 460, ch. 8, pp. 189–206.
- [8] C. Brandstätt, G. Brunekreeft, and K. Jahnke, "How to deal with negative power price spikes? Flexible voluntary curtailment agreements for large-scale integration of wind," *Energy Policy*, vol. 39, no. 6, pp. 3732–3740, Jun. 2011.
- [9] R. Fernandes, I. da Silva, and M. Oleskovicz, "Load profile identification interface for consumer online monitoring purposes in smart grids," *IEEE Trans. Ind. Informat.*, vol. 9, no. 3, pp. 1507–1517, Aug. 2013.
- [10] M. A. Lisovich, M. K. Deirdre, and S. B. Wicker, "Inferring personal information from demand-response systems," *IEEE Security Privacy*, vol. 8, no. 1, pp. 11–20, 2010.
- [11] E. Pournaras, M. Warnier, and F. M. T. Brazier, "Local agent-based self-stabilisation in global resource utilisation," *Int. J. Auton. Comput.*, vol. 1, no. 4, pp. 350–373, Dec. 2010.
- [12] R. Giancarlo, G. Lo Bosco, and L. Pinello, "Distance functions, clustering algorithms and microarray data analysis," in *Learning and Intelligent Optimization*, C. Blum and R. Battiti, Eds. Berlin, Germany: Springer-Verlag, 2010, vol. 6073, pp. 125–138.
- [13] A. Sfetsos and C. Siriopoulos, "Time series forecasting of averaged data with efficient use of information," *IEEE Trans. Syst., Man, Cybern. A, Syst., Humans*, vol. 35, no. 5, pp. 738–745, 2005.
- [14] C. Borges, Y. Penya, and I. Fernandez, "Evaluating combined load forecasting in large power systems and smart grids," *IEEE Trans. Ind. Informat.*, vol. 9, no. 3, pp. 1570–1577, Aug. 2013.
- [15] E. Pournaras, "Multi-level reconfigurable self-organization in overlay services," Ph.D. dissertation, Dept. Multi-actor Syst., Delft Univ. Technol., Delft, The Netherlands, Mar. 2013.
- [16] E. Pournaras, M. Warnier, and F. M. T. Brazier, "Adaptation strategies for self-management of tree overlay networks," in *Proc. 11th IEEE/ACM Int. Conf. Grid Comput. (Grid'10)*, Oct. 2010, pp. 401–409.
- [17] R. Chang and C. Lu, "Feeder reconfiguration for load factor improvement," in *Proc. Power Eng. Soc. Winter Meet.*, 2002, vol. 2, pp. 980–984.
- [18] D. J. Hammerstrom, "Part I. Olympic Peninsula Project," Pacific Northwest Nat. Lab., Richland, WA, USA, Tech. Rep. NNL-17167, Oct. 2007.
- [19] A. K. Jain, "Data clustering: 50 years beyond k-means," *Pattern Recognit. Lett.*, vol. 31, no. 8, pp. 651–666, 2010.
- [20] W. Galuba, K. Aberer, Z. Despotovic, and W. Kellerer, "ProtoPeer: A P2P toolkit bridging the gap between simulation and live deployment," in *Proc. 2nd Int. Conf. Simul. Tools Techn. (ICST'09)*, Mar. 2009, pp. 1–9.
- [21] E. Pournaras, M. Warnier, and F. M. T. Brazier, "Self-optimised tree overlays using proximity-driven self-organised agents," in *Complex Intelligent Systems and Their Applications*. New York, NY, USA: Springer, Aug. 2010, vol. 41, ch. 7, pp. 137–161.
- [22] J. Quinlan, *C4.5: Programs for Machine Learning*. San Mateo, CA, USA: Morgan Kaufmann, 1993.



**Evangelos Pournaras** received the B.Sc. degree in technology education and digital systems from the University of Piraeus, Piraeus, Greece; the M.Sc. degree in internet computing from the University of Surrey, Guildford, Surrey, U.K.; and the Ph.D. degree from the Delft University of Technology, Delft, The Netherlands, in 2013.

He worked as a Visiting Researcher with the École Polytechnique Fédérale de Lausanne (EPFL), Lausanne, Switzerland, and as an Intern with IBM T.J. Watson Research Center, Armonk, NY, USA.

He is a Postdoctoral Researcher with the Network Architectures and Services Group, Department of Computer Science and Engineering, Delft University of Technology. He serves the program committees of several international conferences and has several publications in area of self-management of large-scale decentralized systems, such as smart grids. He is currently working on the RobuSmart project focusing on managing robustness in smart grids.



**Matteo Vasirani** received the M.Sc. degree in computer science from the University of Modena, Reggio Emilia, Italy, in 2004, and the Ph.D. degree in artificial intelligence from Rey Juan Carlos University, Madrid, Spain, in 2009.

He was an Assistant Professor and Associate Director for Training and Promotion, Centre for Intelligent Information Technologies (CETINIA), Rey Juan Carlos University. He is a Research Associate with the Distributed Information Systems Laboratory, École Polytechnique Fédérale de Lausanne,

Lausanne, Switzerland. He is the author of several publications in journals and international conferences, and currently leads a European project (Wattalyst) working on agent-based techniques and intelligent data analysis for residential demand–response programs.



**Robert E. Kooij** received the M.Sc. and Ph.D. degrees (both *cum laude*) in mathematics from the Delft University of Technology, Delft, The Netherlands, in 1988 and 1993, respectively.

From 1997 to 2003, he was employed with Royal Dutch Telecom (KPN) Research, The Hague, The Netherlands. Since 2003, he has been employed with Netherlands Organisation for Applied Scientific Research (TNO), where he is a Principal Scientist dealing with quality aspects of information and communication technologies (ICT) networks. As Knowledge Research Manager, he is responsible for the program on Critical ICT Infrastructures. Since 2005, he has been part-time affiliated with the Faculty of Electrical Engineering, Mathematics, and Computer Science, Delft University of Technology. Since 2010, he has been a part-time Full Professor with the Chair “Robustness of Complex Networks.”



**Karl Aberer** received the Ph.D. degree in mathematics from the Eidgenössische Technische Hochschule Zürich (ETH), Zurich, Switzerland, in 1991.

From 1991 to 1992, he was a Postdoctoral Fellow with the International Computer Science Institute (ICSI), University of California, Berkeley, CA, USA. In 1992, he joined the Integrated Publication and Information Systems Institute (IPSI), Forschungszentrum Informationstechnik GmbH (GMD), Darmstadt, Germany, where he

was leading the research division Open Adaptive Information Management Systems. Since 2000, he was a Full Professor for Distributed Information Systems with the École Polytechnique Fédérale de Lausanne (EPFL), Lausanne, Switzerland. From 2004 to 2011, he was consulting for the Swiss government on research and science policy as a member of the Swiss Research and Technology Council (SWTR). From 2005 to 2012, he was the Director of the Swiss National Research Center for Mobile Information and Communication Systems (NCCR-MICS, [www.mics.ch](http://www.mics.ch)), Lausanne. Since September 2012, he has been the Vice-President of EPFL responsible for information systems. His research interests include decentralization and self-organization in information systems with applications in peer-to-peer search, semantic web, trust management, and mobile and sensor networks.

Dr. Aberer is a Member of the editorial boards of the *International Journal on Very Large Data Bases (VLDB)*, the *ACM Transaction on Autonomous and Adaptive Systems*, and the *World Wide Web Journal*.